Atmospheric Chemistry and Physics

Ref: egusphere-2025-2204

Long–term Trends in $PM_{2.5}$ Chemical Composition and Its Impact on Aerosol Properties: Field Observations from 2007 to 2020 in Pearl River Delta, South China

Response Letter to Reviewer's Comments

Dear reviewer:

We sincerely thank you for your time and valuable comments. We have carefully revised the manuscript to improve its clarity and enhance the readers' understanding. Our point-by-point responses are marked in blue and the corresponding changes to the original text are shown below each response. We hope that these revisions adequately address the comments and concerns.

Comment 1. There is a lack of placing into context the findings in this study to other prior studies that have found similar phenomena. Specifically, I noted that the discussion of the impact of aerosol water on the organic aerosol species lacks many references to other studies that initially identified aerosol water as a major influencing factor on organic aerosol concentrations, some of which are from over 10 years ago. This is especially true in the paragraph starting in Line 302 and Section 3.3.

Response: Thanks for reminding this and providing valuable literature. It is important to discuss the studies with similar findings, which can also support the conclusion of our study. We have added the related discussion and cited these references in the revised manuscript (Introduction, Section 3.2.2 and 3.3).

Acidity, defined as pH, is a crucial aerosol property that affects human health, ecosystems and climate (Nenes et al., 2020; Su et al., 2020; Song et al., 2024). Low pH increases solubility of metals associated with mineral dust (Fang et al., 2017). Previous epidemiological studies revealed that exposure to acidic $PM_{2.5}$ is relevant to high mortality and morbidity (Gwynn et al., 2000; Zhang et al., 2022a). Additionally, aerosol acidity and ALWC regulate the gas–particle partitioning of semi–volatile compounds, as well as chemical reaction rates in the atmosphere, highlighting their importance for the atmospheric lifetime of pollutants (Pye et al., 2020; Nenes et al., 2021). Aqueous uptake is an important formation pathway for secondary species (Yu et al., 2005; Kawamura and Bikkina, 2016; Liu et al., 2021). As an abundant medium, ALWC can enhance their formation (Carlton and Turpin, 2013; Zheng et al., 2015). By modifying particle ability to be activated into cloud condensation nuclei (CCN), ALWC can further influence the climate system (Duan et al., 2019). Furthermore, Attwood et al. (2014) reported that the variation in ALWC changed the aerosol light extinction and radiative forcing. Therefore, it is necessary to explore the trends of pH and ALWC under the change in $PM_{2.5}$ chemical composition.

SOA is formed through the oxidation of VOCs, followed by partitioning from gas phase to

particle phase. Although VOCs emission kept rising (Bian et al., 2019; Guo et al., 2024) and concentration of O_3 fluctuated (Fig. S12a) during the past decade, SOA declined significantly (–0.74 μg m^{-3} yr^{-1}, $p < 0.01$). Previous studies have demonstrated that ALWC is a key factor driving the partitioning of organic compounds from the gas phase into the particle phase, thereby promoting SOA formation (Ervens et al., 2011; Carlton and Turpin, 2013). Nguyen et al. (2015) observed concurrent decreasing trends in ALWC and OC in the Southeast U.S., and further suggested that anthropogenic inorganic species modulated SOA formation through ALWC effects. In addition, higher aerosol acidity has been shown to enhance SOA formation via acid-catalyzed reactions (Surratt et al., 2007). These findings indicated that the reduction in SOA during our study period aerosol could be attributed to the changes in acidity and ALWC, which will be discussed in Sect. 3.3. As SOA accounted for more than 50% of OM, more efforts are needed to reduce it.

The rapid reduction in hygroscopic components, especially SO_4^{2-}, led to the decline of ALWC (Attwood et al., 2014). Our results showed that ALWC decreased from 20.5 ± 10.0 to 9.5 ± 3.9 μg m^{-3}, at a rate of –1.1 μg m^{-3} yr^{-1} ($p < 0.01$). Unexpectedly, low ALWC was observed in 2008 when SIA concentrations, which enhance the hygroscopicity of particulate matter, were at very high levels. It might be associated with low RH (Table S1). To eliminate the influence of changes in meteorological conditions, we used annual average temperature and RH during the entire campaign period as input to recalculate pH and ALWC. The results showed a clear enhancement of ALWC in 2008 (Fig. S17), and the upward trend in pH and downward trend in ALWC still persisted. This demonstrated the long–term trends of pH and ALWC were mainly driven by the changes in chemical composition of $PM_{2.5}$. As we discussed in Sect. 3.2.2, ALWC exhibited positive correlations with SOR and NOR. This indicated a positive feedback mechanism in which the reductions in hygroscopic components (e.g., sulfate and nitrate) leaded to lower ALWC, thereby suppressing SIA formation. Many studies have demonstrated that high aerosol acidity, ALWC, and O_3 will facilitate SOA formation (Ervens et al., 2011; Carlton and Turpin, 2013; Nguyen et al., 2015; Zhang et al., 2022b; Ma et al., 2024; Zhang et al., 2024).

Comment 2. I noted that the timeframe of the study includes 2020, yet there is no acknowledgement of the potential impacts of this anomalous year on the long-term trend. The authors need to at least make note of the fact that large emissions changes during 2020 may impact the trend, and where possible, quantify the uncertainty that brings to their analysis.

Response: Thanks for this comment. Previous studies have reported a dramatic decline in anthropogenic pollutants during the COVID-19 lockdowns. Therefore, it is necessary to evaluate the impact of this anomalous period on the trends of $PM_{2.5}$ and its chemical composition. We used the slopes derived from Theil–Sen regression to represent the change rates for different components, and performed a sensitivity analysis of long-term trends with and without the year 2020. The estimated uncertainties ranged from 1% to 20% (see below, Table S2), indicating that including this anomalous year in the trend analysis would not introduce large bias on the overall long-term trends.

We showed the sensitive analysis results in supplement and clarified it in the revised manuscript (Section 3.1).

Annual average concentrations of $PM_{2.5}$ and its chemical composition are presented in Fig. 2a and Table S1. It is worth noting that the year 2020 was characterized by unprecedented emission reductions associated with COVID-19-related lockdowns (Wang et al., 2021), which may have temporarily affected the trends in $PM_{2.5}$ and its chemical composition. As shown in Table S2, a sensitivity analysis was conducted to evaluate the uncertainty introduced by including 2020 in the trend analysis. The sensitive analysis suggested that this anomalous year would not introduce large bias on the overall long-term trends. From 2007 to 2020, $PM_{2.5}$ concentrations exhibited a significant decline from 87.1 ± 15.5 μg m^{-3} to 34.0 ± 11.3 μg m^{-3}, at a rate of –4.0 μg m^{-3} yr^{-1} ($p < 0.01$). This trend aligns with the previous results from meta–analysis (–3.9 μg m^{-3} yr^{-1}) and regional simulation (–4.0 μg m^{-3} yr^{-1}) in the PRD (Zhang et al., 2019; Yan et al., 2020), affirming WQS can serve as a regional background site.

Table S2. Sensitivity analysis of long-term trends with and without the year 2020.

	Slope (with 2020)	Slope (without 2020)	Uncertainty
$PM_{2.5}$	-4.0 **	-4.2 **	4%
OM	-1.70 **	-1.91 **	12%
EC	-0.23 **	-0.25 **	9%
SO_4^{2-}	-1.13 **	-1.21 **	7%
NO_3^-	-0.40 **	-0.47 **	18%
NH_4^+	-0.31 **	-0.33 **	6%
Cl^-	-0.10 **	-0.10 **	1%
Na^+	-0.05 **	-0.06 **	20%
K^+	-0.10 **	-0.12 **	16%
Mg^{2+}		-0.01 *	
Ca^{2+}	-0.06 *	-0.06 *	3%

One asterisk, two asterisks denote p value < 0.05, 0.01, respectively. Blank cells denote p value > 0.05. The uncertainty was calculated as: $\boldsymbol{Uncertainty} = \frac{|Slope_{with} - Slope_{without}|}{|Slope_{with}|}$.

Comment 3. "EC is a product of carbon fuel-based combustion processes and is exclusively associated with primary emission…" I am a bit confused on this paragraph. Are the authors referring to the EC measured by the OC/EC analyzer? If so, then this statement needs more clarification and discussion of uncertainties. Instrument-measured OC and EC are determined optically, and are thus more operational definitions than true determinants of carbon sources. The cutoff temperatures between OC and EC varies by instrument type and network protocol followed,

and errors for the cutoff tend to be large. The authors should specify what temperatures were used for their analysis, and quantify where possible the uncertainty associated with their chosen protocol.
Response: We thank the reviewer for raising this important point regarding the definition and measurement of OC/EC and providing valuable references. To minimize potential measurement biases and enhance data comparability, we used the same thermal-optical carbon analyzer and followed the same analytical protocol throughout the study. We have added related clarification and discussion of uncertainties in the Methodology (Section 2.2 and 2.3).

Due to the fact that organic carbon (OC) and elemental carbon (EC) are operationally defined and highly sensitive to analytical conditions, different thermal-optical methods may lead to discrepancies in the OC/EC measurements (Khan et al., 2012; Giannoni et al., 2016). To minimize potential measurement biases and enhance data comparability, we used the same thermal-optical carbon analyzer and followed the same analytical protocol throughout the study. Specifically, the OC and EC were determined by the thermal–optical transmittance (TOT) method (NIOSH, 1999) using an OC/EC analyzer (Sunset Laboratory Inc., USA), with a punch (1.5 × 1.0 cm) of the sampled filters. The samples were analyzed by stepwise heating. First, the sample was heated sequentially to 870 °C (310 °C for 60 s, 475 °C for 60 s, 620 °C for 60 s, and 870 °C for 90 s) under a pure helium (He) atmosphere, during which OC was volatilized, and a portion of it underwent pyrolysis, forming pyrolyzed carbon. After cooling, the sample was reheated under a 2% O_2/He atmosphere up to 920 °C (625 °C for 30 s, 700 °C for 30 s, 775 °C for 30 s, 850 °C for 30 s, and 920 °C for 30 s) to oxidize EC and pyrolyzed carbon.

Prior to OC/EC analysis, we calibrated the instrument using glucose standards at multiple concentrations. The instrument responses were highly linear ($R^2 > 0.99$) and the relative errors between measured and prepared concentrations were within ± 5%. The method detection limits (MDLs) were 0.01–0.05 μg m^{-3} for the OC, EC, cations, and anions. Ion balance was employed as a quality control check in the anion/cation analysis. A significant linear correlation ($R^2 = 0.97$) was observed between anions and cations, with a slope of 0.82 for all $PM_{2.5}$ samples. This slope, being close to unity, indicated that all the significant ions were resolved.

Comment 4. Please provide more details on the EC-tracer method and how it differs from your Bayesian Inference Approach. In addition, please describe the Bayesian approach in more detail. What is the significance of the K values?
Response: The EC-tracer method assumes that elemental carbon (EC) originates from primary combustion sources and uses a fixed $(OC/EC)_{pri}$ ratio to estimate primary organic carbon (POC), from which secondary organic carbon (SOC) is obtained by subtracting POC from total OC. Although a few methods have been proposed to estimate the $(OC/EC)_{pri}$, such as minimum (OC/EC) and minimum R squared method, the choice of this $(OC/EC)_{pri}$ value is often arbitrary and could introduce significant uncertainties. Bayesian Inference Approach adopts a probabilistic framework that combines prior knowledge (in the form of prior distributions of the K values) with observational

data (OC, EC, and secondary inorganic aerosol species like sulfate) to estimate the source contributions to OC. The Bayesian Inference Approach assumes that observed OC is a linear combination of contributions from POC and SOC tracers (e.g., EC and SO_4^{2-}), and it uses the Markov Chain Monte Carlo (MCMC) technique to derive posterior distributions for the K values. This probabilistic treatment allows the model to update parameter estimates based on actual measurements. The K values represent the proportionality constants that link OC to its respective tracers (e.g., K_{EC} for EC-to-POC and K_{SO42-} for sulfate-to-SOC). We have added related introduction into section 2.4.

EC is a product of carbon fuel–based combustion processes and is exclusively associated with primary emissions, whereas OC can be formed from both direct emissions and secondary pathways. Differentiation between primary organic carbon (POC) and secondary organic carbon (SOC) is indispensable for probing atmospheric aging processes of organic aerosols, but all available methods for estimating POC and SOC are highly uncertain. The EC–tracer method was widely used to estimate POC and SOC (Turpin and Huntzicker, 1991; 1995). Given that EC is emitted exclusively from primary combustion sources (e.g., fossil fuel and biomass burning), it is commonly used as a tracer for POC. Under this assumption, POC is estimated by multiplying EC by a representative primary OC/EC ratio, and SOC is determined as the residual between total OC and estimated POC (eq. 1 and 2). One of the most commonly used approaches to determine $(OC/EC)_{pri}$ is the minimum OC/EC ratio approach (Castro et al., 1999), which assumes that the lowest observed OC/EC value corresponds to conditions dominated by primary emissions with negligible SOC formation. In addition, Pio et al. (2011) recommended using the 5% percentile of observed OC/EC values instead, and Wu and Yu (2016) proposed minimum R squared (MRS) method to obtain $(OC/EC)_{pri}$.

$$POC = \left(\frac{OC}{EC}\right)_{pri} \times EC \quad (1)$$

$$SOC = OC - POC \quad (2)$$

However, a previous study revealed that EC–tracer method relied on the fixed $(OC/EC)_{pri}$ and tended to overestimate SOC (Kim et al., 2012). Recently, Liao et al. (2023) proposed Bayesian Inference (BI) approach and suggested it more accurately estimated POC and SOC compared to the conventional method, such as EC–tracer method, minimum ratio value, minimum R squared, and multiple linear regression. The BI approach adopts a probabilistic framework that combines prior knowledge (in the form of prior distributions of the K values) with observational data (OC, EC, and secondary inorganic aerosol) to estimate the source contributions to OC. The BI model assumes that observed OC is a linear combination of contributions from POC and SOC tracers (e.g., EC and SO_4^{2-}), and it uses the Markov Chain Monte Carlo (MCMC) technique to derive posterior distributions for the K values. This treatment allows the model to update parameter estimates based on actual measurements and offers more flexibility while having greater computational complexity. In this study, we used Bayesian Inference Approach which has the convenience of relying only on the commonly available mass concentrations of EC and SO_4^{2-} to estimate POC and SOC. They can be calculated as following:

$$SOC = K_{EC} \times EC + K_{SO42-} \times SO_4^{2-} \quad (3)$$

$$POC = OC - SOC \quad (4)$$

Where K_{EC} and K_{SO42-} are parameters calculated by Bayesian Inference Approach in R language, the details can be found in previous research (Liao et al., 2023). The K values represent the proportionality constants that link OC to its respective tracers (e.g., K_{EC} for EC-to-POC and K_{SO42-} for sulfate-to-SOC). The variations of K value are shown in Fig. S2. Given intense photochemical reactions and larger fractions of aged aerosols in the PRD, a higher conversion factor of 2.4 was employed to convert SOC to SOA (Yan et al., 2020).

Comment 5. It is unclear why the conversion from SOC to SOA is needed.

Response: We appreciate the reviewer's comment. The conversion from secondary organic carbon (SOC) to secondary organic aerosol (SOA) is necessary because SOC represents only the carbonaceous portion of the organic aerosol, while SOA includes the entire mass of organic compounds formed through secondary processes, including associated non-carbon atoms (e.g., hydrogen, oxygen, nitrogen). To better evaluate the atmospheric mass loading of organic aerosols and their mass proportions in $PM_{2.5}$, it is important to quantify SOA in terms of mass concentration ($\mu g\ m^{-3}$), not just carbon content. A conversion factor (commonly referred to as the organic mass to organic carbon ratio) is thus applied. In this study, we adopted a factor of 2.4 based on previous literature (Yan et al., 2020), which reflects the higher oxidation state of SOA formed under intense photochemical activity in the PRD region. This factor accounts for the added oxygenated functional groups in aged aerosols and is consistent with values used in other field studies in similar environments.

Comment 6. The authors refer to annual average PM2.5 concentrations, but earlier state that most measurements were done from October to December. Are the concentrations shown here true annual averages, or are they the averages from October to December (wintertime)? How many of the samples fall outside this October to December range?

Response: We thank the reviewer for the insightful comment. Indeed, all of the samples in this study were collected during the October to December, which corresponds to the winter season. Therefore, the $PM_{2.5}$ concentrations and chemical compositions presented in this paper should be interpreted as representative of the wintertime conditions rather than true annual averages. We acknowledge this seasonal limitation and have revised the relevant descriptions in the revised manuscript to avoid confusion.

Comment 7. There are several undefined acronyms (POA, SOA, SIA) – this is true in other areas of the manuscript as well (ALWC, SOR, NOR). These need to be defined at their first usage.

Response: We thank the reviewer for pointing this out. We have carefully reviewed the entire manuscript and ensured that all acronyms are defined at their first occurrence. Specifically, the

following acronyms have now been clearly defined:

- POA: Primary Organic Aerosol
- SOA: Secondary Organic Aerosol
- SIA: Secondary Inorganic Aerosol
- ALWC: Aerosol Liquid Water Content
- SOR: Sulfur Oxidation Ratio
- NOR: Nitrogen Oxidation Ratio

We have also checked the revised manuscript to confirm that no undefined acronyms remain. All abbreviations are now properly introduced upon first use to improve clarity and readability.

Comment 8. Where the authors state that the Bayesian Inference approach is more reliable. On what basis are you making this claim? To what are you comparing the approaches to determine reliability?
Response: We thank the reviewer for pointing this out. We conducted correlation analysis between oxalic acid (a typical and abundant organic secondary molecular marker) and SOC estimated by Bayesian Inference approach, as well as SOC estimated by EC-tracer method. The result showed that the correlation between oxalic acid and SOC (BI approach) ($r = 0.62$, $p < 0.05$) was stronger than correlation between oxalic acid and SOC (EC-tracer method) ($r = 0.54$, $p < 0.05$), which indicated the estimation from BI approach was more reliable. We showed this in Fig. S5 (see below) in supplement but not mentioned in manuscript, which could lead to confusion. We have added related description in the revised manuscript.

Our result showed that the average concentration of SOC estimated by the Bayesian Inference (BI) approach was ~30% lower than that by the EC–tracer method. In addition, the correlation between oxalic acid (a typical secondary organic molecular marker) and SOC estimated by the BI approach ($r = 0.62$, $p < 0.05$) was stronger than that with SOC estimated by the EC-tracer method ($r = 0.54$, $p < 0.05$), indicating the estimation from BI approach was more reliable (Fig. S5).

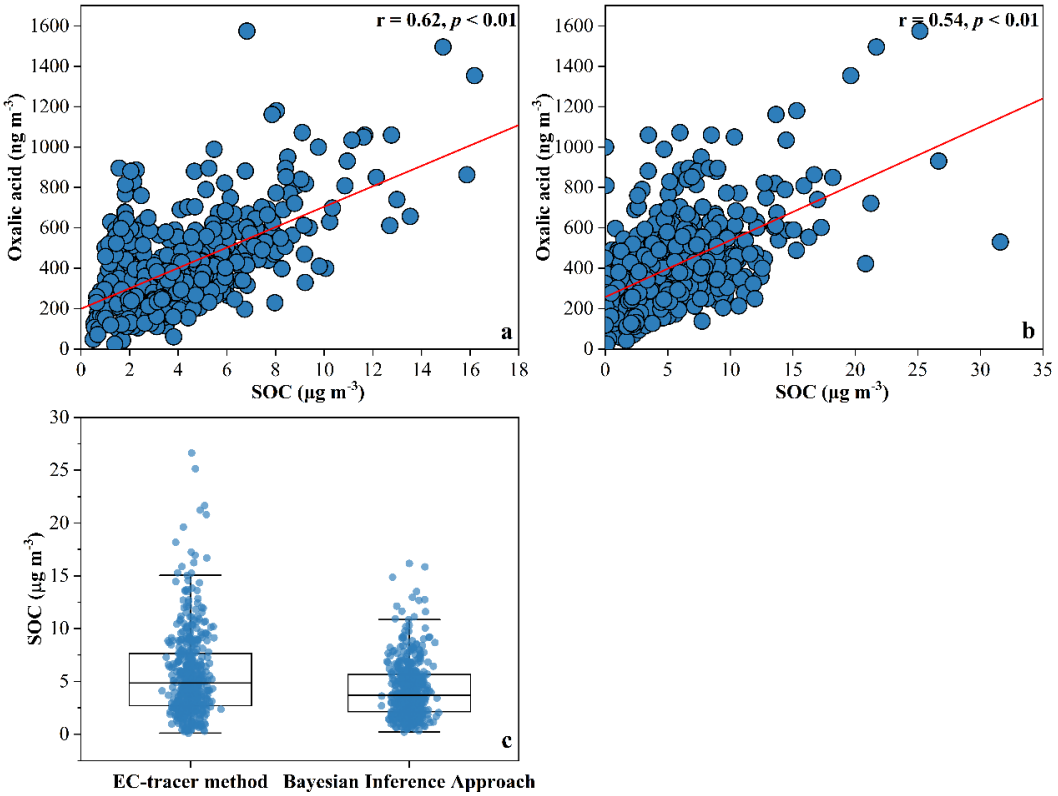

Figure S5. Oxalic acid, a typical secondary organic molecular tracer, exhibited a significant correlation ($p < 0.01$) with SOC estimated using both Bayesian Inference Approach (a) and EC–tracer method (b). The Pearson's correlation coefficient for the Bayesian Inference Approach (0.62) was higher than that for the EC–tracer method (0.54), suggesting that SOC derived from the Bayesian Inference Approach might be more reliable. In addition, the average SOC concentration estimated by the Bayesian Inference Approach (4.1 ± 2.6 μg m^{-3}) was lower and more than that by the EC–tracer method (5.8 ± 4.2 μg m^{-3}) (c).

Comment 9. What control measures have been put in place for biomass burning and dust?

Response: We thank the reviewer for the valuable question. In the past decades, several control measures have been implemented in the Pearl River Delta (PRD) region to reduce emissions from biomass burning and dust sources. The main measures and relevant policy frameworks are summarized below:

Control category	Main Measures	Sources
Biomass burning	Based on the types and distribution of crop straw, an integrated plan for comprehensive straw utilization has been formulated and steadily implemented. The focus is placed on strictly banning open burning and promoting the comprehensive utilization of surplus straw. These measures aim to enhance the efficient use of straw resources and address the issues of resource waste and environmental pollution caused by improper disposal and illegal burning.	2
	Accelerate the establishment and improvement of policies and mechanisms for the comprehensive utilization of biomass waste, and effectively control the uncontrolled burning of biomass waste in rural areas and around urban fringes.	6
	Open burning is strictly prohibited, and the responsibility for straw burning control must be rigorously implemented at the municipal, county, and township government levels. Effective measures should be taken to strengthen the supervision and management of straw burning bans.	8

Dust	Strengthen comprehensive control of urban fugitive dust throughout the entire process. In each city, designated dust control zones should cover more than 80% of the built-up area, and dust pollution must be effectively managed. Dust control at material storage and handling sites must be enhanced. Facilities storing or piling dust-prone materials such as coal, gangue, cinder, fly ash, sand, and soil should be equipped with enclosed structures, spraying systems, and surface solidification measures. At construction sites, strict implementation of enclosure measures, proper disposal of construction waste, and water spraying for dust suppression is required.	1, 3
	Strengthen the control of dust pollution from construction activities and roadways. Promote the application of dust suppression technologies at construction sites, and establish dynamic databases of dust sources along with online monitoring systems for particulate matter. Actively promote green construction practices by requiring construction units to implement measures such as site enclosure, installation of vehicle washing facilities, and road pavement hardening, while strictly prohibiting open-air operations. In the main urban areas of each city, the transportation of construction waste and powdery materials should gradually be carried out in enclosed vehicles equipped with satellite positioning systems.	4
	Strengthen the regulation of spillage from vehicles transporting construction waste, earth and rock, and industrial raw and auxiliary materials in urban areas. Enclosed transport vehicles or tightly covered truck beds should be used, and all transport activities must follow designated routes and time schedules. Road cleaning practices should be improved by promoting standardized operations and increasing the rate of mechanized street sweeping and water spraying. The mechanized cleaning rate of roads in built-up urban areas should exceed 85%.	5, 7
	All prefecture-level and above cities are required to establish citywide online monitoring and management platforms for construction site dust emissions. The use of fully enclosed vehicles for transporting construction waste and powdery materials should be promoted, and the phasing out and replacement of outdated transport vehicles is encouraged.	8

No.	Release year	Main documents
1	2005	Notice on the Issuance of the “Pearl River Delta Environmental Protection Plan Outline (2004–2020)”
2	2008	Circular on Forwarding the Opinions of the General Office of the State Council on Accelerating the Comprehensive Utilization of Crop Straw
3	2010	Notice on the Issuance of the “Integrated Environmental Protection Plan for the Pearl River Delta (2009–2020)”
4	2014	Notice of the Guangdong Provincial People's Government on Issuing the Guangdong Province Air Pollution Prevention and Control Action Plan (2014–2017)
5	2016	Notice of the Guangdong Provincial Department of Environmental Protection on Issuing the “13th Five-Year Plan for Environmental Protection in Guangdong Province”
6	2016	Notice of the Guangdong Provincial Department of Environmental Protection on Issuing the “13th Five-Year Plan for Environmental Protection in Guangdong Province”

7	2017	Notice of the General Office of the Guangdong Provincial People's Government on Issuing the Enhanced Measures and Task Allocation Plan for Air Pollution Prevention and Control in Guangdong Province
8	2018	Notice of the Guangdong Provincial People's Government on Issuing the "Guangdong Province Blue Sky Protection Campaign Implementation Plan (2018–2020)"

Comment 10. Nitrate accumulation would be more impacted by temperature than NO2 concentrations.

Response: Thanks for pointing this. We acknowledge that nitrate accumulation is strongly influenced by temperature and relative humidity, and we have clarified this point in the revised manuscript. In addition, we have included an estimate of the potential underestimation caused by the volatilization of ammonium nitrate. Here, we want to discuss the differences between intercepts observed in the NO_3^-/NO_2 regression and those in SO_4^{2-}/SO_2 regression. When NO_2 level is low, the formation of HNO_3, gaseous precursor of NO_3^- is suppressed. Therefore, the reaction in eq. 2 tends to proceed to the left. This indicates that more NO_3^- will partition into gas phase, leading to less NO_3^- accumulates in particle phase. Thus, the intercepts observed in the NO_3^-/NO_2 regression were lower.

$$OH\ (g) + NO_2\ (g) + M \rightarrow HNO_3\ (g) + M \quad \text{(eq. 1)}$$

$$HNO_3(g) + NH_3\ (g) \leftrightarrow NO_3^-(aq) + NH_4^+(aq) \quad \text{(eq. 2)}$$

SO_4^{2-} showed a clear decrease at a rate of –1.13 μg m^{-3} yr^{-1} (–10% yr^{-1}, $p < 0.01$), whereas NO_3^- and NH_4^+ showed moderate declines (–0.40 μg m^{-3} yr^{-1}, –6% yr^{-1}; –0.31 μg m^{-3} yr^{-1}, –6% yr^{-1}, respectively, $p < 0.05$). Previous studies reported that the volatilization of ammonium nitrate during sampling can cause negative mass artifacts, leading to the underestimation of both NO_3^- (8%–16%) (Chow et al., 2005) and NH_4^+ (10%–28%) (Yu et al., 2006). The volatilization is highly dependent on the changes in relative humidity (RH) and temperature. However, such losses are expected to be systematic over time and therefore are unlikely to significantly affect their general trends in this study, because our measurements were conducted in the same season. Strong correlations between SO_4^{2-}/SO_2, as well as between NO_3^-/NO_2 were observed (Fig. S9), suggesting that reductions of SO_4^{2-} and NO_3^- were mainly driven by their gaseous precursors. With RH rising, the slopes of SO_4^{2-}/SO_2, as well as NO_3^-/NO_2, increased, indicating enhanced conversion of primary pollutants to secondary species. The generally lower intercepts observed in the NO_3^-/NO_2 regression compared to those in the SO_4^{2-}/SO_2 regression can be explained by the semi-volatile nature of nitrate (Yu et al., 2006). The formation of HNO_3, gaseous precursor of NO_3^-, is suppressed under low NO_2 level. Therefore, the reaction in eq. 2 tends to proceed to the left. This facilitates partitioning of NO_3^- into gas phase, leading to less accumulation of NO_3^- in particle phase. In contrast, sulfate is the least volatile among all the inorganic aerosol components (Kang et al., 2022), allowing it to be stably retained in the particle phase once formed.

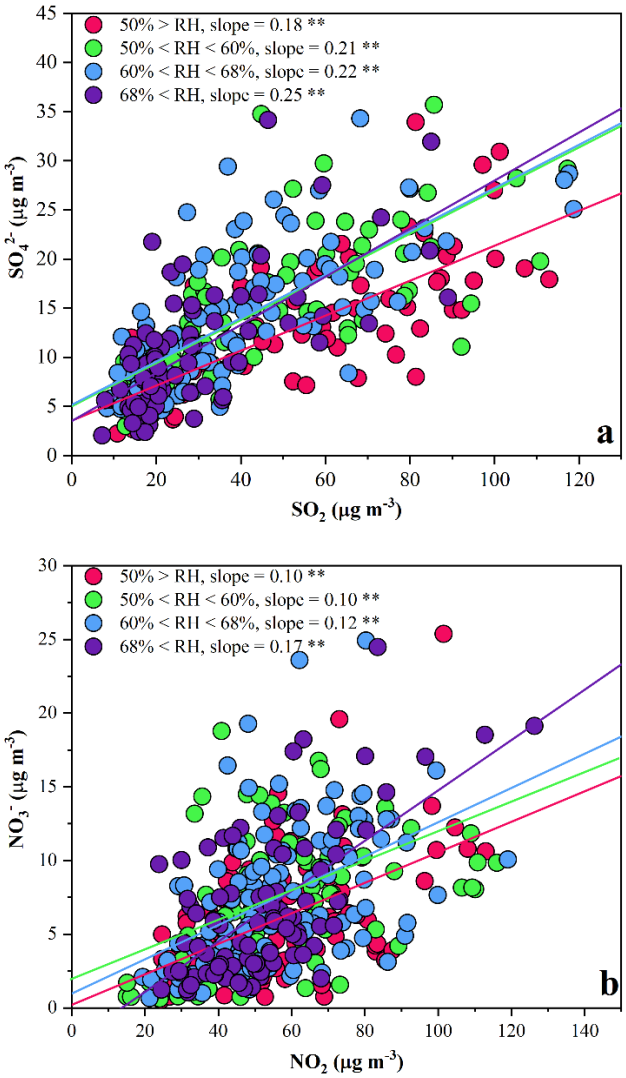

Figure S9. Correlations between SO_4^{2-}/SO_2 (a), as well as NO_3^-/NO_2 (b). Two asterisks denote *p* value less than 0.01.

Comment 11. The authors should specify which IMPROVE extinction equation they are using. There is an updated one from 2023 (see https://vista.cira.colostate.edu/Improve/wp-content/uploads/2023/10/IMPROVE_Data_User_Guide_24October2023.pdf, Section 8.1). Is that the equation used here? In addition, what is the local parameter scheme?

Response: Thanks for pointing this. It is necessary to illustrate which IMPROVE equation was used in this study. To estimate the light extinction coefficient (bext), the first Interagency Monitoring of Protected Visual Environments (IMPROVE) equation was developed by the U.S. National Park Service with support from the U.S. Environmental Protection Agency (EPA) (Malm et al., 1994; EPA, 2003), but this equation tended to underestimate/overestimate the highest/lowest bext values. Consequently, the revised IMPROVE equation was then proposed (Malm and Hand, 2007; Pitchford et al., 2007). Here, we used the revised one proposed in 2007:

$$bext \approx 2.2 \times f_S(RH) \times [Small\ Ammonium\ Sulfate] + 4.8 \times f_L(RH) \times [Large\ Ammonium\ Sulfate] +$$

$2.4 \times f_S(RH) \times [Small\ Ammonium\ Nitrate] + 5.1 \times f_L(RH) \times [Large\ Ammonium\ Nitrate]$
$+ 2.8 \times [Small\ Organic\ Mass] + 6.1 \times [Large\ Organic\ Mass] +$
$10 \times [Elemental\ Carbon] + 1 \times [Fine\ Soil] + 1.7 \times f_{SS}(RH) \times [Sea\ Salt] +$
$0.6 \times [Coarse\ Mass] + Rayleigh\ Scattering\ (Site\ Specific) + 0.33 \times [NO_2\ (ppb)]$

We have added related introduction in the revised manuscript.

Because the scattering/absorbing efficiency (MSE/MAE) in the revised IMPROVE equation is an approximation based on measurements from clean areas. In addition, the calculation of hygroscopic growth factor (f(RH)) in the revised equation depends on relative humidity (RH) and particle size distribution (or aerosols mass), but does not account for the chemical composition in aerosols, which has been shown to significantly affect f(RH) (Li et al., 2021). These simplifications could lead to large discrepancies in polluted regions. In this study, we adopted the MSE/MAE obtained in the PRD region and calculated f(RH) based on $PM_{2.5}$ chemical composition in the PRD. Then we used them to replace the corresponding parameters in the revised IMPROVE equation, which was called local parameter scheme.

Chemical composition in $PM_{2.5}$ also affects atmospheric visibility through light scattering and absorption. Light scattering is dominated by hydrophilic components, such as organic mass (OM), $(NH_4)_2SO_4$, and NH_4NO_3, while light absorption is largely driven by light–absorbing carbon (Wang et al., 2012). To estimate the light extinction coefficient (b_{ext}), the first Interagency Monitoring of Protected Visual Environments (IMPROVE) equation was developed by the U.S. National Park Service with support from the U.S. Environmental Protection Agency (EPA) (Malm et al., 1994; EPA, 2003), but this equation tended to underestimate/overestimate the highest/lowest b_{ext} values. Consequently, the revised IMPROVE equation was then proposed (Malm and Hand, 2007; Pitchford et al., 2007). However, the scattering/absorbing efficiency (MSE/MAE) in the revised equation is an approximation based on measurements from clean areas. In addition, the calculation of hygroscopic growth factor (f(RH)) in the revised equation depends on relative humidity (RH) and particle size distribution (or aerosols mass), but does not account for the chemical composition in aerosols, which has been shown to significantly affect f(RH) (Li et al., 2021). These simplifications could lead to large discrepancies in polluted regions. For instance, the deviations between observed and estimated b_{ext} values were reported as 15%, 36%, and 37% in Xi'an, Shanghai, and Guangzhou, respectively (Jung et al., 2009; Cao et al., 2012; Cheng et al., 2015). Thus, region-specific adjustments are necessary to reflect the impact of particle composition on these parameters from site to site.

We adopted MSE/MAE suggested by Fu et al. (2016), as well as relationship between chemical composition and f(RH) suggested by Li et al. (2021), to reconstruct b_{ext} (herein called local parameter scheme) using equations (5-8).

$$b_{ext} = 6.5 \times [OM] + 2.6 \times f(\mathrm{RH}) \times [AS] + 2.4 \times f(\mathrm{RH}) \times [AN] + 7.3 \times f(\mathrm{RH})_{ss} \times [SS] + 7.7 \times [LAC] \quad (5)$$

$$f(\mathrm{RH}) = [(1-RH)/(1-\mathrm{RH}_{ref})]^{-\gamma} \quad (6)$$

$$\gamma = 0.48 \times F + 0.59 \quad (7)$$

$$F = (OC+EC)/(OC+EC+SO_4^{2-}+NO_3^-+NH_4^+) \quad (8)$$

Comment 12. Does the IMPROVE equation overestimate, or does the local parameterization underestimate? It is not clear that this can be said with any certainty. It is probably better to just state the differences between the methods.

Response: We thank the reviewer for the valuable suggestion. Due to lack of real measurements of bext in the PRD during our study period, it does not make sense to say the revised IMPROVE equation tend to overestimate bext or the local parameter scheme underestimate it. We have changed the statement in the revised manuscript.

We also calculated b_{ext} by the revised IMPROVE equation and compared to the local parameter scheme (Fig. S21). Generally, b_{ext} estimated by the revised IMPROVE equation (335.72 ± 219.64 Mm^{-1}) was significantly higher than that estimated by local parameter scheme (262.67 ± 143.82 Mm^{-1}). We further investigated this discrepancy under different pollution levels. With the improvement in air quality, the difference between the two schemes narrowed gradually ($p < 0.01$).

Comment 13. Figure 3: What do the error bars represent?

Response: Thank you for comment. The error bars in Figure 3 represent the standard deviation of the total concentration, calculated as the sum of primary and secondary species. We have added this in revised manuscript.

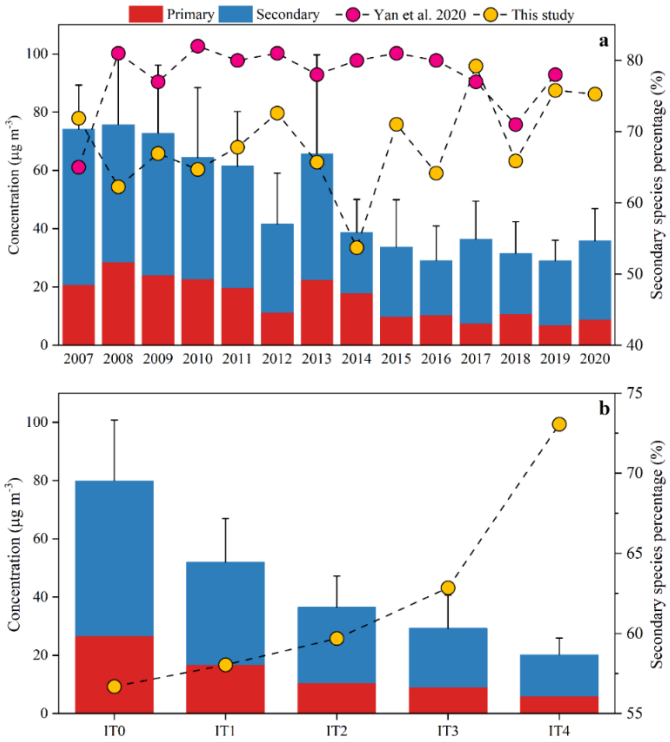

Figure 3. The variations in primary and secondary species during 2007–2020 (a) and their variations under different pollutants levels (b). Bars represent concentrations of them and circles represent the mass proportion of secondary species in $PM_{2.5}$. Secondary species (account for 54%–79%) dominated over primary species. The proportion of secondary species increased from 57% to 73% with improvement of air quality

(From IT0 to IT4). The error bars in Figure 3 represent the standard deviation of the total concentration, calculated as the sum of primary and secondary species.

Comment 14. Text S2 should be moved to the main document.

Response: Thanks for your suggestion. The calculation of aerosol pH and ALWC is a important part of our results. It indeed should be illustrated in the main document.

Comment 15. Figure S6 may benefit from an additional line showing the uncorrected changes in Cl-.

Response: Thanks for suggestion. We have added the line on the chart.

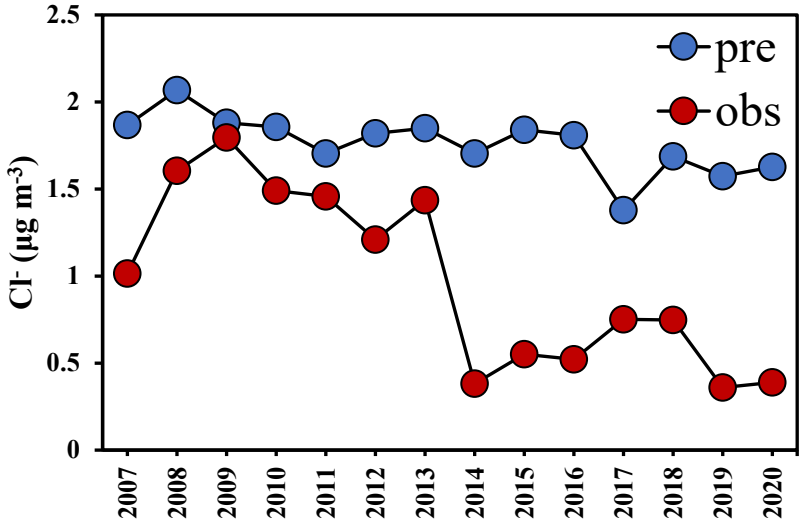

Figure S8. The observation (red) and prediction (blue) concentration of Cl^-. After eliminating variations in anthropogenic sources on Cl^-. It decreased slightly at a rate of –2% yr^{-1} during 2007-2020 (blue).

Comment 16. Figure S7: The colors of the lines do not match the colors in the legend.

Response: Thanks for reminding. We have corrected that.

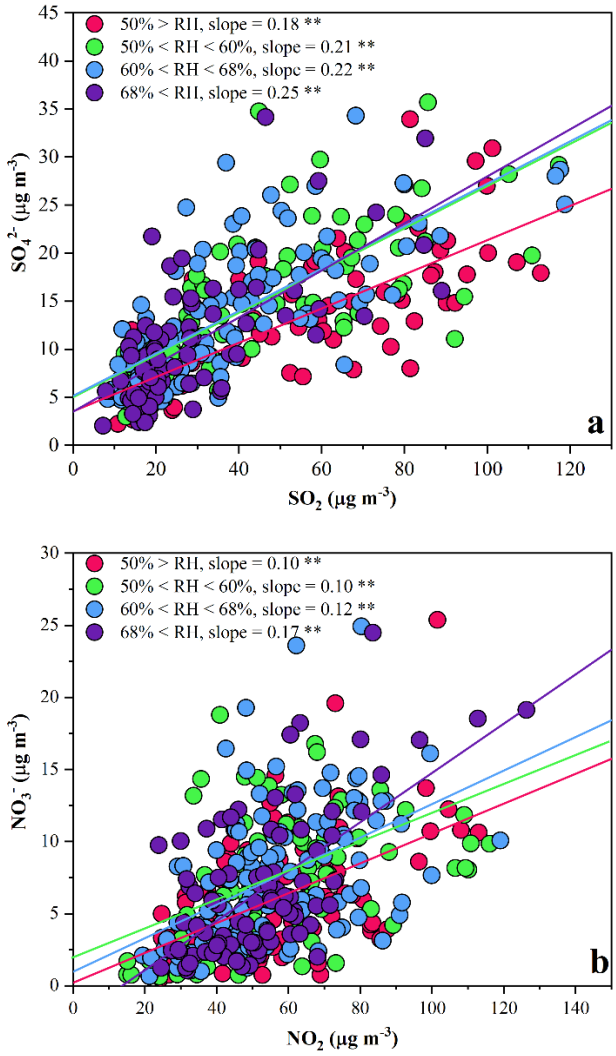

Comment 17. Figure S8: Define SOR.

Response: Thanks for reminding. We have added defination of SOR and NOR in the revised supplement.

References:

Attwood, A. R., Washenfelder, R. A., Brock, C. A., Hu, W., Baumann, K., Campuzano-Jost, P., Day, D. A., Edgerton, E. S., Murphy, D. M., Palm, B. B., McComiskey, A., Wagner, N. L., de Sá, S. S., Ortega, A., Martin, S. T., Jimenez, J. L., and Brown, S. S.: Trends in sulfate and organic aerosol mass in the Southeast U.S.: Impact on aerosol optical depth and radiative forcing, Geophys. Res. Lett., 41, 7701-7709, https://doi.org/https://doi.org/10.1002/2014GL061669, 2014.

Bian, Y. H., Huang, Z. J., Ou, J. M., Zhong, Z. M., Xu, Y. Q., Zhang, Z. W., Xiao, X., Ye, X., Wu, Y. Q., Yin, X. H., Li, C., Chen, L. F., Shao, M., and Zheng, J. Y.: Evolution of anthropogenic air pollutant emissions in Guangdong Province, China, from 2006 to 2015, Atmos. Chem. Phys., 19, 11701-11719, https://doi.org/10.5194/acp-19-11701-2019, 2019.

Cao, J.-j., Wang, Q.-y., Chow, J. C., Watson, J. G., Tie, X.-x., Shen, Z.-x., Wang, P., and An, Z.-s.: Impacts of aerosol compositions on visibility impairment in Xi'an, China, Atmos. Environ., 59, 559-566, https://doi.org/10.1016/j.atmosenv.2012.05.036, 2012.

Carlton, A. G. and Turpin, B. J.: Particle partitioning potential of organic compounds is highest in the Eastern US and driven by anthropogenic water, Atmos. Chem. Phys., 13, 10203-10214, https://doi.org/10.5194/acp-13-10203-2013, 2013.

Castro, L. M., Pio, C. A., Harrison, R. M., and Smith, D. J. T.: Carbonaceous aerosol in urban and rural European atmospheres: estimation of secondary organic carbon concentrations, Atmos. Environ., 33, 2771-2781, https://doi.org/https://doi.org/10.1016/S1352-2310(98)00331-8, 1999.

Cheng, Z., Jiang, J., Chen, C., Gao, J., Wang, S., Watson, J. G., Wang, H., Deng, J., Wang, B., Zhou, M., Chow, J. C., Pitchford, M. L., and Hao, J.: Estimation of Aerosol Mass Scattering Efficiencies under High Mass Loading: Case Study for the Megacity of Shanghai, China, Environ. Sci. Technol., 49, 831-838, https://doi.org/10.1021/es504567q, 2015.

Chow, J. C., G., W. J., H., L. D., and and Magliano, K. L.: Loss of PM2.5 Nitrate from Filter Samples in Central California, Journal of the Air & Waste Management Association, 55, 1158-1168, https://doi.org/10.1080/10473289.2005.10464704, 2005.

Duan, J., Lyu, R., Wang, Y., Xie, X., Wu, Y., Tao, J., Cheng, T., Liu, Y., Peng, Y., Zhang, R., He, Q., Ga, W., Zhang, X., and Zhang, Q.: Particle Liquid Water Content and Aerosol Acidity Acting as Indicators of Aerosol Activation Changes in Cloud Condensation Nuclei (CCN) during Pollution Eruption in Guangzhou of South China, Aerosol Air Qual. Res., 9, 2662-2670, https://doi.org/10.4209/aaqr.2019.09.0476, 2019.

EPA: Guidance for Tracking Progress Under the Regional Haze Rule, https://www.epa.gov/visibility/guidance-tracking-progress-under-regional-haze-rule, last access: 2 July 2025.

Ervens, B., Turpin, B. J., and Weber, R. J.: Secondary organic aerosol formation in cloud droplets and aqueous particles (aqSOA): a review of laboratory, field and model studies, Atmos. Chem. Phys., 11, 11069-11102, https://doi.org/10.5194/acp-11-11069-2011, 2011.

Fang, T., Guo, H. Y., Zeng, L. H., Verma, V., Nenes, A., and Weber, R. J.: Highly Acidic Ambient Particles, Soluble Metals, and Oxidative Potential: A Link between Sulfate and Aerosol Toxicity, Environ. Sci. Technol., 51, 2611-2620, https://doi.org/10.1021/acs.est.6b06151, 2017.

Fu, X., Wang, X., Hu, Q., Li, G., Ding, X., Zhang, Y., He, Q., Liu, T., Zhang, Z., Yu, Q., Shen, R., and Bi, X.: Changes in visibility with PM2.5 composition and relative humidity at a background site in the Pearl River Delta region, J. Environ. Sci., 40, 10-19, https://doi.org/10.1016/j.jes.2015.12.001, 2016.

Giannoni, M., Calzolai, G., Chiari, M., Cincinelli, A., Lucarelli, F., Martellini, T., and Nava, S.: A comparison between thermal-optical transmittance elemental carbon measured by different protocols in PM2.5 samples, Sci. Total Environ., 571, 195-205, https://doi.org/https://doi.org/10.1016/j.scitotenv.2016.07.128, 2016.

Guo, Q., Wang, Y., Zheng, J., Zhu, M., Sha, Q. e., and Huang, Z.: Temporal evolution of speciated volatile organic compound (VOC) emissions from solvent use sources in the Pearl River Delta Region, China (2006–2019), Sci. Total Environ., 933, 172888, https://doi.org/10.1016/j.scitotenv.2024.172888, 2024.

Gwynn, R. C., Burnett, R. T., and Thurston, G. D.: A time-series analysis of acidic particulate matter and daily mortality and morbidity in the Buffalo, New York, region, Environ. Health Perspect., 108, 125-133, https://doi.org/10.1289/ehp.00108125, 2000.

Jung, J., Lee, H., Kim, Y. J., Liu, X., Zhang, Y., Gu, J., and Fan, S.: Aerosol chemistry and the effect of aerosol water content on visibility impairment and radiative forcing in Guangzhou during the 2006 Pearl River Delta campaign, J. Environ. Manage., 90, 3231-3244, https://doi.org/10.1016/j.jenvman.2009.04.021, 2009.

Kang, H. G., Kim, Y., Collier, S., Zhang, Q., and Kim, H.: Volatility of Springtime ambient organic aerosol derived with thermodenuder aerosol mass spectrometry in Seoul, Korea, Environ. Pollut., 304,

119203, https://doi.org/10.1016/j.envpol.2022.119203, 2022.

Kawamura, K. and Bikkina, S.: A review of dicarboxylic acids and related compounds in atmospheric aerosols: Molecular distributions, sources and transformation, Atmos. Res., 170, 140-160, https://doi.org/10.1016/j.atmosres.2015.11.018, 2016.

Khan, B., Hays, M. D., Geron, C., and Jetter, J.: Differences in the OC/EC Ratios that Characterize Ambient and Source Aerosols due to Thermal-Optical Analysis, Aerosol Sci. Technol., 46, 127-137, https://doi.org/10.1080/02786826.2011.609194, 2012.

Kim, W., Lee, H., Kim, J., Jeong, U., and Kweon, J.: Estimation of seasonal diurnal variations in primary and secondary organic carbon concentrations in the urban atmosphere: EC tracer and multiple regression approaches, Atmos. Environ., 56, 101-108, https://doi.org/10.1016/j.atmosenv.2012.03.076, 2012.

Li, J., Zhang, Z., Wu, Y., Tao, J., Xia, Y., Wang, C., and Zhang, R.: Effects of chemical compositions in fine particles and their identified sources on hygroscopic growth factor during dry season in urban Guangzhou of South China, Sci. Total Environ., 801, 149749, https://doi.org/10.1016/j.scitotenv.2021.149749, 2021.

Liao, K., Wang, Q., Wang, S., and Yu, J. Z.: Bayesian Inference Approach to Quantify Primary and Secondary Organic Carbon in Fine Particulate Matter Using Major Species Measurements, Environ. Sci. Technol., 57, 5169-5179, https://doi.org/10.1021/acs.est.2c09412, 2023.

Liu, T. Y., Chan, A. W. H., and Abbatt, J. P. D.: Multiphase Oxidation of Sulfur Dioxide in Aerosol Particles: Implications for Sulfate Formation in Polluted Environments, Environ. Sci. Technol., 55, 4227-4242, https://doi.org/10.1021/acs.est.0c06496, 2021.

Ma, F., Wang, H., Ding, Y., Zhang, S., Wu, G., Li, Y., Gong, D., Ristovski, Z., He, C., and Wang, B.: Amplified Secondary Organic Aerosol Formation Induced by Anthropogenic–Biogenic Interactions in Forests Around Megacities, J. Geophys. Res.: Atmos., 129, e2024JD041679, https://doi.org/10.1029/2024JD041679, 2024.

Malm, W. C. and Hand, J. L.: An examination of the physical and optical properties of aerosols collected in the IMPROVE program, Atmos. Environ., 41, 3407-3427, https://doi.org/https://doi.org/10.1016/j.atmosenv.2006.12.012, 2007.

Malm, W. C., Sisler, J. F., Huffman, D., Eldred, R. A., and Cahill, T. A.: Spatial and seasonal trends in particle concentration and optical extinction in the United States, 99, 1347-1370, https://doi.org/10.1029/93JD02916, 1994.

Nenes, A., Pandis, S. N., Weber, R. J., and Russell, A.: Aerosol pH and liquid water content determine when particulate matter is sensitive to ammonia and nitrate availability, Atmos. Chem. Phys., 20, 3249-3258, https://doi.org/10.5194/acp-20-3249-2020, 2020.

Nenes, A., Pandis, S. N., Kanakidou, M., Russell, A. G., Song, S., Vasilakos, P., and Weber, R. J.: Aerosol acidity and liquid water content regulate the dry deposition of inorganic reactive nitrogen, Atmos. Chem. Phys., 21, 6023-6033, https://doi.org/10.5194/acp-21-6023-2021, 2021.

Nguyen, T. K. V., Capps, S. L., and Carlton, A. G.: Decreasing Aerosol Water Is Consistent with OC Trends in the Southeast U.S, Environ. Sci. Technol., 49, 7843-7850, https://doi.org/10.1021/acs.est.5b00828, 2015.

NIOSH: NIOSH Method 5040 Issue 3 (Interim): Elemental Carbon (diesel exhaust) https://hero.epa.gov/hero/index.cfm/reference/details/reference_id/156811, last access: 14 July, 2025.

Pio, C., Cerqueira, M., Harrison, R. M., Nunes, T., Mirante, F., Alves, C., Oliveira, C., Sanchez de la Campa, A., Artíñano, B., and Matos, M.: OC/EC ratio observations in Europe: Re-thinking the approach for apportionment between primary and secondary organic carbon, Atmos. Environ., 45, 6121-6132, https://doi.org/https://doi.org/10.1016/j.atmosenv.2011.08.045, 2011.

Pitchford, M., Maim, W., Schichtel, B., Kumar, N., Lowenthal, D., and Hand, J.: Revised algorithm for estimating light extinction from IMPROVE particle speciation data, Journal of the Air & Waste Management Association (1995), 57, 1326-1336, https://doi.org/10.3155/1047-3289.57.11.1326, 2007.

Pye, H. O. T., Nenes, A., Alexander, B., Ault, A. P., Barth, M. C., Clegg, S. L., Collett Jr, J. L., Fahey, K. M., Hennigan, C. J., Herrmann, H., Kanakidou, M., Kelly, J. T., Ku, I. T., McNeill, V. F., Riemer, N., Schaefer, T., Shi, G., Tilgner, A., Walker, J. T., Wang, T., Weber, R., Xing, J., Zaveri, R. A., and Zuend, A.: The acidity of atmospheric particles and clouds, Atmos. Chem. Phys., 20, 4809-4888, https://doi.org/10.5194/acp-20-4809-2020, 2020.

Song, X., Wu, D., Su, Y., Li, Y., and Li, Q.: Review of health effects driven by aerosol acidity: Occurrence and implications for air pollution control, Sci. Total Environ., 955, 176839, https://doi.org/10.1016/j.scitotenv.2024.176839, 2024.

Su, H., Cheng, Y., and Pöschl, U.: New Multiphase Chemical Processes Influencing Atmospheric Aerosols, Air Quality, and Climate in the Anthropocene, Acc. Chem. Res., 53, 2034-2043, https://doi.org/10.1021/acs.accounts.0c00246, 2020.

Surratt, J. D., Lewandowski, M., Offenberg, J. H., Jaoui, M., Kleindienst, T. E., Edney, E. O., and Seinfeld, J. H.: Effect of Acidity on Secondary Organic Aerosol Formation from Isoprene, Environ. Sci. Technol., 41, 5363-5369, https://doi.org/10.1021/es0704176, 2007.

Turpin, B. J. and Huntzicker, J. J.: Secondary formation of organic aerosol in the Los Angeles basin: A descriptive analysis of organic and elemental carbon concentrations, Atmospheric Environment. Part A. General Topics, 25, 207-215, https://doi.org/10.1016/0960-1686(91)90291-E, 1991.

Turpin, B. J. and Huntzicker, J. J.: Identification of secondary organic aerosol episodes and quantitation of primary and secondary organic aerosol concentrations during SCAQS, Atmos. Environ., 29, 3527-3544, https://doi.org/10.1016/1352-2310(94)00276-Q, 1995.

Wang, N., Xu, J. W., Pei, C. L., Tang, R., Zhou, D. R., Chen, Y. N., Li, M., Deng, X. J., Deng, T., Huang, X., and Ding, A. J.: Air Quality During COVID-19 Lockdown in the Yangtze River Delta and the Pearl River Delta: Two Different Responsive Mechanisms to Emission Reductions in China, Environ. Sci. Technol., 55, 5721-5730, https://doi.org/10.1021/acs.est.0c08383, 2021.

Wang, X. M., Ding, X., Fu, X. X., He, Q. F., Wang, S. Y., Bernard, F., Zhao, X. Y., and Wu, D.: Aerosol scattering coefficients and major chemical compositions of fine particles observed at a rural site hit the central Pearl River Delta, South China, J. Environ. Sci., 24, 72-77, https://doi.org/10.1016/s1001-0742(11)60730-4, 2012.

Wu, C. and Yu, J. Z.: Determination of primary combustion source organic carbon-to-elemental carbon (OC/EC) ratio using ambient OC and EC measurements: secondary OC-EC correlation minimization method, Atmos. Chem. Phys., 16, 5453-5465, https://doi.org/10.5194/acp-16-5453-2016, 2016.

Yan, F. H., Chen, W. H., Jia, S. G., Zhong, B. Q., Yang, L. M., Mao, J. Y., Chang, M., Shao, M., Yuan, B., Situ, S., Wang, X. M., Chen, D. H., and Wang, X. M.: Stabilization for the secondary species contribution to PM2.5 in the Pearl River Delta (PRD) over the past decade, China: A meta-analysis, Atmos. Environ., 242, https://doi.org/10.1016/j.atmosenv.2020.117817, 2020.

Yu, J. Z., Huang, X.-F., Xu, J., and Hu, M.: When Aerosol Sulfate Goes Up, So Does Oxalate: Implication for the Formation Mechanisms of Oxalate, Environ. Sci. Technol., 39, 128-133, https://doi.org/10.1021/es049559f, 2005.

Yu, X.-Y., Lee, T., Ayres, B., Kreidenweis, S. M., Malm, W., and Collett, J. L.: Loss of fine particle ammonium from denuded nylon filters, Atmos. Environ., 40, 4797-4807, https://doi.org/https://doi.org/10.1016/j.atmosenv.2006.03.061, 2006.

Zhang, Q., Meng, X., Shi, S., Kan, L., Chen, R., and Kan, H.: Overview of particulate air pollution and human health in China: Evidence, challenges, and opportunities, The Innovation, 3, 100312, https://doi.org/10.1016/j.xinn.2022.100312, 2022a.

Zhang, Q., Zheng, Y. X., Tong, D., Shao, M., Wang, S. X., Zhang, Y. H., Xu, X. D., Wang, J. N., He, H., Liu, W. Q., Ding, Y. H., Lei, Y., Li, J. H., Wang, Z. F., Zhang, X. Y., Wang, Y. S., Cheng, J., Liu, Y., Shi, Q. R., Yan, L., Geng, G. N., Hong, C. P., Li, M., Liu, F., Zheng, B., Cao, J. J., Ding, A. J., Gao, J., Fu, Q. Y., Huo, J. T., Liu, B. X., Liu, Z. R., Yang, F. M., He, K. B., and Hao, J. M.: Drivers of improved PM2.5 air quality in China from 2013 to 2017, PNAS, 116, 24463-24469, https://doi.org/10.1073/pnas.1907956116, 2019.

Zhang, S., Gong, D., Wu, G., Li, Y., Ding, Y., Wang, B., and Wang, H.: Molecular characteristics and formation mechanisms of biogenic secondary organic aerosols in the mountainous background atmosphere of southern China, Atmos. Environ., 329, 120540, https://doi.org/10.1016/j.atmosenv.2024.120540, 2024.

Zhang, Y.-Q., Ding, X., He, Q.-F., Wen, T.-X., Wang, J.-Q., Yang, K., Jiang, H., Cheng, Q., Liu, P., Wang, Z.-R., He, Y.-F., Hu, W.-W., Wang, Q.-Y., Xin, J.-Y., Wang, Y.-S., and Wang, X.-M.: Observational Insights into Isoprene Secondary Organic Aerosol Formation through the Epoxide Pathway at Three Urban Sites from Northern to Southern China, Environ. Sci. Technol., 56, 4795-4805, https://doi.org/10.1021/acs.est.1c06974, 2022b.

Zheng, B., Zhang, Q., Zhang, Y., He, K. B., Wang, K., Zheng, G. J., Duan, F. K., Ma, Y. L., and Kimoto, T.: Heterogeneous chemistry: a mechanism missing in current models to explain secondary inorganic aerosol formation during the January 2013 haze episode in North China, Atmos. Chem. Phys., 15, 2031-2049, https://doi.org/10.5194/acp-15-2031-2015, 2015.